Conference on Modelling Fluid Flow (CMFF'25)
The 19th International Conference on Fluid Flow Technologies
Budapest, Hungary, August 26-August 29, 2025

NUMERICAL INVESTIGATION OF A LIFTED METHANE/AIR JET FLAME USING STOCHASTIC MAP-BASED TURBULENCE MODELING

Tommy Starick[1], Heiko Schmidt[2,3]

[1] Corresponding Author. Chair of Numerical Fluid and Gas Dynamics, Institute of Transport Technology, Brandenburg University of Technology (BTU) Cottbus-Senftenberg, Siemens-Halske-Ring 15a, 03046 Cottbus, Germany. Tel.: +49 355 69 4813, Fax: +49 355 69 4891, E-mail: Tommy.Starick@b-tu.de
[2] Chair of Numerical Fluid and Gas Dynamics, Institute of Transport Technology, Brandenburg University of Technology (BTU) Cottbus-Senftenberg, Siemens-Halske-Ring 15a, 03046 Cottbus, Germany. Tel.: +49 355 69 4874, Fax: +49 355 69 4891, E-mail: Heiko.Schmidt@b-tu.de
[3] Scientific Computing Lab (SCL), Energy Innovation Center (EIZ), Brandenburg University of Technology (BTU) Cottbus-Senftenberg, 03046 Cottbus, Germany.

ABSTRACT

This numerical study investigates a lifted methane/air jet flame in a vitiated coflow by means of the map-based, stochastic one-dimensional turbulence (ODT) model. The dimensional reduction of ODT allows for simulations with affordable computational costs and provides nonetheless full-scale resolution along a notional line of sight crossing the turbulent flow field. The considered Cabra burner configuration consists of a jet flame issuing from a central nozzle into a vitiated coflow of hot combustion products. Radial and centerline profiles for mixture fraction, temperature and selected species mass fractions obtained from ODT using a reduced and detailed reaction mechanism are in appropriate agreement with the existing experimental measurements. A two-dimensional illustration of the autoignition index is given, which enables the distinction between autoignition and propagation driven reaction zones. Additionally, the sensitivity of the jet combustion to velocity and temperature variations is investigated. Considering the reduced order of ODT and the sensitivity of the subtle interactions of the hot coflow with the cold jet on the entire reaction process, ODT is able to predict the flow characteristics and reasonably matches the experimental data. As a consequence, ODT is an efficient and alternative model for turbulent reactive flow simulations.

Keywords: autoigniton, lifted jet flame, methane/air combustion, ODT, one-dimensional turbulence, stochastic turbulence modeling

NOMENCLATURE

C	$[-]$	ODT model parameter - turbulence intensity
D	$[m]$	jet diameter
E_{kin}	$[J]$	available kinetic energy
E_{vp}	$[J]$	energetic viscous penalty
M_k	$[\frac{kg}{mol}]$	molecular weight of species k
P	$[Pa]$	thermodynamic pressure
R_u	$[\frac{J}{K \cdot mol}]$	universal gas constant
T	$[K]$	thermodynamic temperature
V_k	$[\frac{m}{s}]$	diffusion velocity of species k
X_k	$[-]$	mole fraction of species k
Y_k	$[-]$	mass fraction of species k
Z	$[-]$	ODT model parameter - viscous penalty
Δt_{sample}	$[s]$	sampling time interval
$\dot{w}_k$	$[\frac{kg}{m^3 \cdot s}]$	reaction rate of species k
f	$[-]$	mixture fraction
l	$[m]$	eddy size
r	$[m]$	radial position
r_0	$[m]$	eddy location
t	$[s]$	simulation time
u_i	$[\frac{m}{s}]$	velocity component
z	$[m]$	downstream position
β	$[-]$	ODT model parameter - large eddy suppression
λ	$[\frac{1}{s \cdot m^2}]$	eddy rate
μ	$[\frac{kg}{m \cdot s}]$	dynamic viscosity
ρ	$[\frac{kg}{m^3}]$	density of the gas mixture
τ	$[s]$	eddy event time scale

1. INTRODUCTION

Recirculating burners are a special type of burner that reinjects part of the hot exhaust gases back into the combustion process. This technology is used to enhance combustion efficiency, reduce pollutant emissions (especially nitrogen oxides), control flame temperature and to get wider fuel and operation flexibility. By recirculating the exhaust gases, the oxygen concentration in the combustion chamber is lowered, resulting in slower and more uniform com-

bustion. Recirculating burners are widely used in industrial heating processes, power plants, and chemical processing applications where optimized energy utilization and emission reduction are required.

The numerical study of this special type of burner is challenging due to the recirculation of hot combustion products. Vitiated coflow burners exhibit similar characteristics in terms of chemical kinetics, heat transfer, and molecular transport as recirculating burners, where the stabilized flame is lifted from the burner by increased jet or coflow velocity. However, they avoid the complexities associated with recirculating fluid mechanics, as demonstrated in the experimental measurements of Cabra et al. [1].

Despite the simplified consideration of a recirculating burner as a vitiated coflow burner, the accurate representation of the turbulent reactive flow is a standing challenge in numerical fluid dynamics. The small-scale interactions of the hot coflow with the unburnt jet flow are crucial for the entire reaction of the jet and necessitate a full resolution of all relevant time and length scales in order to completely capture the state-space statistics.

Direct numerical simulation (DNS) would be the ideal method for turbulent reactive flows, as it provides complete resolution of the flow without modeling errors. However, for most industrial applications, DNS remains prohibitively computationally expensive and is therefore also not a feasible option in the foreseeable future [2].

To enable the numerical study of turbulent reactive flows despite computational limitations, turbulence closure models are commonly applied. In contrast to the full resolution of DNS, large-eddy simulation (LES) and Reynolds-averaged Navier-Stokes (RANS) approaches resolve the flow only in a filtered or averaged sense, which reduces the computational effort in the desired way. To compensate for the limited state-space information of the scalar composition, these lower-fidelity models often incorporate transported probability density function (PDF) methods [3].

The considered Cabra burner configuration, consisting of a jet flame issuing from a central nozzle into a vitiated coflow of hot combustion products, represents an important test case and has been investigated by a variety of LES [4, 5, 6, 7] and RANS [1, 8, 9, 10] simulations.

These studies show that the averaged or filtered results generally are in reasonable agreement with the experimental measurements and are able to capture key combustion characteristics. However, despite the use of filtering or averaging, LES and RANS simulations remain computationally demanding due to the need for resolving the expensive chemistry alongside of the transported PDF approach. As a result, their applicability for extensive sensitivity analyses or comprehensive parameter studies is limited.

Reduced order turbulence and mixing models offer an alternative approach, significantly lowering computational costs compared to DNS while preserving fundamental physical conservation principles and accurately capturing turbulent flow phenomenology.

In reduced order stochastic mixing and turbulence models, map-based transformations are applied in one-dimensional domains to mimic the effects of turbulent mixing and advection. Notable representatives are the linear eddy model (LEM) [11] and the hierarchical parcel swapping (HiPS) model [12], both mixing models, and the one-dimensional turbulence (ODT) model [13], all developed by A. Kerstein. These models efficiently utilize available computational resources through dimensional order reduction while fully resolving the entire range of scales within the one-dimensional domain. This makes LEM, HiPS and ODT particularly well-suited for applications where small-scale interactions between advection, diffusion, and reaction play a crucial role.

The main objective of this work is the scale-resolving, pyhsics-based, yet computationally efficient numerical investigation of the Cabra jet flame in a vitiated coflow. The results from the ODT model are thoroughly compared with the experimental data from Cabra et al. [1]. Additionally, the autoignition index is evaluated, and the sensitivity of the lift off height to variations in jet velocity and coflow temperature is examined.

The paper is structured as follows: Section 2 provides a more detailed description of the ODT model formulation. Section 3 describes the flow configuration for the considered methane/air jet flame in a vitiated coflow. Section 4 presents and discusses the model results, followed by concluding remarks.

2. ODT MODEL FORMULATION

The one-dimensional turbulence (ODT) model offers a significantly reduced numerical framework compared to DNS and LES, enabling full-scale resolution in the radial direction of the jet. This makes ODT an ideal tool for the numerical study of a lifted methane/air jet flame in a vitiated coflow. For this round jet flame, a cylindrical ODT formulation is used to account for the geometric proportions. This formulation is detailed in Lignell et al. [14].

ODT employs a stochastic, map-based approach to represent turbulent advection. The diffusion and reaction kinetics along the one-dimensional domain are modeled through the temporal advancement of deterministic evolution equations. Unlike averaged or filtered simulation approaches, such as RANS or LES, ODT integrates molecular processes (e.g., chemical reactions and diffusive transport) without introducing additional approximations or modeling assumptions.

The effects of three-dimensional turbulence are incorporated into ODT through the use of stochastic *eddy events*. These eddy events directly represent the turbulent transport characteristics affecting fluid

properties along the simulated one-dimensional domain. Each eddy event modifies property fields by applying a *triplet map*.

A triplet map is a measure-preserving transformation rule that ensures the continuity of advected fields, leading to the steepening of local property gradients [14, 15]. The map operates by taking a line segment $[r_0, r_0 + l]$ with a randomly selected eddy location r_0 and size l, shrinking it to a third of its original length, and then placing three copies of the segment on the original domain. The middle copy is reversed. The features of the triplet map in the cylindrical ODT formulation can be reviewed in [14].

Eddy events are sampled in time using a marked Poisson process, with assumed Probability Density Functions (PDFs) for eddy locations r_0 and sizes l. This process replicates the statistics of turbulent flows on average by oversampling the number of events representing turbulent transport, while maintaining a target mean acceptance probability for the eddy events, as discussed in [16] and [14]. The acceptance probability of a particular eddy within a given sampling time interval Δt_{sample} is determined by calculating a rate λ of the eddy candidate.

The eddy rate λ, as shown in Eq. 1, depends on r_0, l, and the eddy event time scale τ. The time scale τ is proportional to the difference between the available kinetic energy E_{kin} in the eddy range and an energetic viscous penalty E_{vp} for suppressing excessively small eddies, as described in [14]. While the energetic viscous penalty does not significantly affect the statistical results, it is beneficial for improving the model's performance.

$$\lambda(r_0, l, \tau) \equiv \frac{C}{l^2 \tau} \sim C\left(E_{kin} - Z E_{vp}\right) \tag{1}$$

C and Z are dimensionless ODT model parameters that are initially calibrated and then remain constant.

Due to its reduced dimensionality, ODT does not capture large-scale coherent structures. Occasionally, during the initial phase, the eddy sampling process may accept unphysically large eddies, which can negatively impact turbulent transport. To prevent this, ODT employs a large eddy suppression mechanism.

This mechanism eliminates eddies whose event time scale is disproportionately larger than the elapsed simulation time t. In general, eddies are only implemented if the following condition

$$\tau \leq \beta t \tag{2}$$

is satisfied, where β is another dimensionless ODT model parameter which is determined beforehand [14].

Eddies are sampled sequentially in time. Once an eddy is implemented, a deterministic catch-up process takes place, advancing the diffusive-reactive transport equations up to the physical time at which the eddy was selected for implementation.

In an open system configuration, such as the lifted jet flame examined in this study, the deterministic evolution follows integral conservation laws based on a Lagrangian ODT formulation, as described in [14].

The integral expressions for the conservation of mass, momentum, and energy are presented below. The mass conservation equation is given as follows.

$$\frac{\mathrm{d}}{\mathrm{d}t} \int \rho r \mathrm{d}r = 0 \tag{3}$$

Here, ρ represents the density of the gas mixture, which is determined by its pressure, temperature, and molecular weight, as described by the ideal gas law.

$$P = \rho R_u T \sum_k \frac{Y_k}{M_k} \tag{4}$$

In this equation, P represents the thermodynamic pressure, which remains constant over time and space in the open jet flame configuration. Additionally, R_u denotes the universal gas constant, T is the temperature of the gas mixture, and Y_k and M_k correspond to the mass fractions and molecular weights of the k-th species that make up the gas mixture, respectively. The species conservation equation is given by following equation.

$$\begin{aligned} \frac{\mathrm{d}}{\mathrm{d}t} \int \rho Y_k r \mathrm{d}r = &- \int \frac{1}{r} \frac{\partial}{\partial r} \left(r \rho V_k Y_k\right) r \mathrm{d}r \\ &+ \int \dot{w}_k r \mathrm{d}r \end{aligned} \tag{5}$$

Here, V_k represents the species diffusion velocities, which require the same modeling approximations as those used in reactive DNS. Similarly, $\dot{w}_k$ denotes the species reaction rates, which are determined by an imported reaction mechanism under specified thermodynamic conditions.

For momentum conservation, we assume that radial transport is dominant and model the diffusion of momentum using the gradient of scalar-modeled shear stresses, following the approach described in [14].

$$\frac{\mathrm{d}}{\mathrm{d}t} \int \rho u_i r \mathrm{d}r = \int \frac{1}{r} \frac{\partial}{\partial r} \left(r \mu \frac{\partial u_i}{\partial r}\right) r \mathrm{d}r \tag{6}$$

In the momentum conservation equation, u_i stands for the three velocity components in the cylindrical system and μ is the dynamic viscosity of the gas mixture. Finally, the energy conservation in the open system is being represented by the conservation of enthalpy h in a zero Mach number limit approximation.

$$\begin{aligned} \frac{\mathrm{d}}{\mathrm{d}t} \int \rho h r \mathrm{d}r = &- \int \frac{1}{r} \frac{\partial}{\partial r} \left(r \rho V_k Y_k h_k\right) r \mathrm{d}r \\ &+ \int \frac{1}{r} \frac{\partial}{\partial r} \left(r \lambda_t \frac{\partial T}{\partial r}\right) r \mathrm{d}r \end{aligned} \tag{7}$$

In this equation, h_k stands for the sensible enthalpy of each k-th species and λ_t is the thermal conductivity of the mixture.

The deterministic time advancement of Eq.3-7 is achieved using a finite volume method (FVM) with first-order time integration. For the analyzed lifted methane/air jet flame, an implicit time integration of Eq.3-7 is applied, where the diffusive flux terms, calculated at the start of each time step, are treated as constants. This approach helps to mitigate the potentially restrictive CFL condition caused by stiff chemistry arising from the species chemical reaction source term. However, this converts the time integration in Eq. 6-7 into an explicit Euler method.

The density, which is updated after time-stepping the enthalpy and species conservation equations (Eq.7 and 5), is computed using Eq.4 based on the new mixture composition and temperature. Once the density is updated, mass conservation is enforced through a conservative remeshing of the grid, following the application of the mass conservation equation [17]. The fluid thermophysical properties are determined using the Cantera software suite, as described in [18].

3. FLOW CONFIGURATION

The Cabra burner configuration [1] consists of a lifted methane/air jet flame in a vitiated coflow generated by an array of lean H_2/air flames. The temperature and species concentrations are considered uniform across the coflow, and the flow field of interest is not influenced by mixing with ambient air [1]. Consequently, the coflow is uniformly initialized in all ODT simulations, and the ambient air is not considered. This results in a pure two-stream configuration. For the base case configuration, the jet and coflow is initialized as specified in Table 1. For every single ODT realization, an instantaneous velocity profile is used generated by ODT pipe flow simulations with a fixed bulk velocity of 100 m/s.

Table 1. Initial conditions for jet and coflow. X, mole fraction; u, velocity; T, temperature; D, diameter;

-	Jet	Coflow
D (mm)	4.57	100
u (m/s)	100	5.4
T (K)	320	1350
X_{CH_4}	0.33	0.0003
X_{O_2}	0.15	0.12
X_{N_2}	0.52	0.73
X_{H_2O}	0.0029	0.15
X_{OH} (ppm)	0.0	200
X_{H_2} (ppm)	100	100

The detailed GRI-Mech 3.0 mechanism [19], which includes 53 species and 325 reactions, along with a reduced reaction mechanism [20] containing 19 species and 15 reactions, is used for the representation of chemical reactions and thermophysical properties.

The ODT results are meant to be compared with the stationary, spatially developing round jet flame measurements from [1]. However, the cylindrical ODT formulation applied here only solves for a radial location, r, and time, t. As a result, a transformation between time and the corresponding downstream position, z, is necessary. This is accomplished by downstream advection of the ODT line using an instantaneous bulk velocity, $\bar{u}$.

$$z(t) = z(t_0) + \int_{t_0}^{t} \bar{u}(t')dt' \tag{8}$$

Here, $z(t_0)$ marks the starting position. The bulk velocity, $\bar{u}$, is calculated by the sum of the free-stream (coflow) velocity, u_∞ , and the ratio of integrated momentum flux to integrated mass flux, as detailed in [21].

$$\bar{u}(t) = u_\infty + \left.\frac{\int_{-\infty}^{\infty} \rho(u-u_\infty)^2 r dr}{\int_{-\infty}^{\infty} \rho(u-u_\infty) r dr}\right|_t \tag{9}$$

For the definition of the mixture fraction, the commonly used Bilger's equation [22] is applied.

4. RESULTS AND DISCUSSION

ODT simulations, using both a reduced and a detailed reaction mechanism, were carried out and compared with the experimental data from Cabra et al. [1]. The Favre-averaging of the ODT results was based on an ensemble size of 1500 realizations. For all presented results, the ODT model parameters C and Z in Eq. 1 were set to $C = 18$ and $Z = 400$, matching the parameters used in the study of a round jet flame with a similar cylindrical formulation by Lignell et al. [14]. Furthermore, a fixed model parameter of $\beta = 1.17$ was used to suppress large eddies during the initial phase of the simulation.

4.1. Centerline profiles

Comparisons are made between the experimental measurements of [1] and ODT simulations using both a reduced and a detailed reaction mechanism. The centerline profiles of the Favre-averaged species mass fractions, temperature, and mixture fraction, along with their corresponding fluctuations, are presented in Figure 1. In these plots, the red and blue curves represent ODT simulation results for the reduced and detailed reaction mechanisms, respectively, while the experimental data from [1] is shown as round black markers.

In the initial phase, up to approximately $z/D \approx 40$, the process is dominated by non-reactive mixing between the cold jet and the hot coflow, leading to a gradual rise in centerline temperature with low fluctuations. This is followed by the flame stabilization phase around $z/D \approx 45$, where a sharp temperature increase, rapid oxygen consumption, hydroxyl

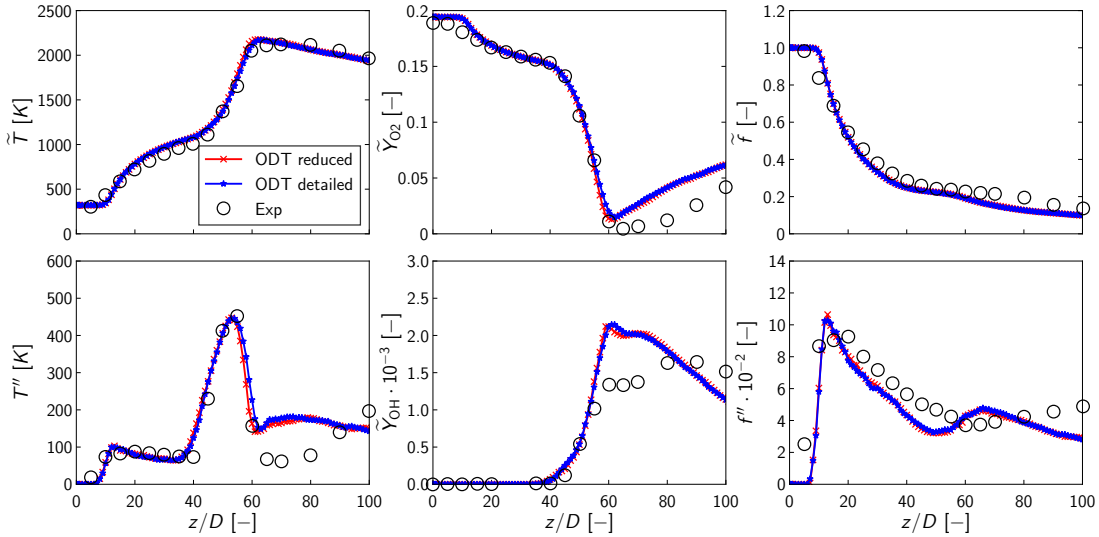

Figure 1. Centerline profiles of Favre-averaged temperature ($\tilde{T}$ and fluctuations T''), species mass fractions (Favre-averaged oxygen mass fraction $\tilde{Y}_{O2}$ and Favre-averaged hydroxyl radical mass fraction $\tilde{Y}_{OH}$), and mixture fraction ($\tilde{f}$ and fluctuations f'') from ODT simulations using a reduced and detailed reaction mechanism for the representation of the methane/air combustion. ODT results are compared to the experimental measurements of [1] (Exp).

radical production, and a peak in temperature fluctuations are observed.

The ODT results for both reaction mechanisms show good agreement with the experimental data, accurately capturing the mixing behavior in the early phase and the subsequent combustion process, as indicated by the steep temperature rise and drop in oxygen mass fraction. Additionally, ODT closely follows the trend and magnitude of the Favre fluctuations observed in the experiments. However, slight overpredictions of the mean mass fractions of O_2 and OH are noted for $z/D > 60$. The differences between the two reaction mechanisms are negligibly small.

4.2. Radial profiles

In addition to the centerline profiles, Figure 2 presents the radial profiles of the Favre-averaged temperature and mixture fraction. Similar to the centerline plots, the red and blue curves represent ODT simulation results using a detailed and a reduced reaction mechanism, respectively. The experimental data for the Favre-averaged values are depicted by round markers.

In the initial phase, where non-reactive mixing occurs between the cold jet and the hot coflow ($z/D = 15$ and $z/D = 30$), the ODT results for both reaction mechanisms show reasonable agreement with the experimental measurements. However, at positions further downstream ($z/D = 50$ and $z/D = 70$), deviations between the ODT results and the experimental data become noticeable. These discrepancies are likely due to the approximation used for determining the downstream position, as described by Eq. 8 and 9.

Unlike the centerline region, where a radially uniform bulk velocity approximation for each time step is more applicable, this approach may not be entirely suitable for the shear region between the cold jet and the hot coflow. A more accurate representation of the downstream advection of the ODT line could potentially be achieved by using a spatial ODT formulation, as suggested in [14].

4.3. Autoignition index

The autoignition index (AI) provides a measure to differentiate between autoignition-driven and propagation-driven reaction zones, as described in [4]. Its definition is based on a reaction rate flux analysis of the HO_2 chemistry. In the detailed GRI-Mech 3.0 mechanism [19], the key reactions governing the consumption of HO_2 play a crucial role in distinguishing between these two types of reaction zones. Specifically, this distinction is made through the following two reactions.

$$HO_2 + H \longleftrightarrow OH + OH \qquad [R46]$$

$$HO_2 + OH \longleftrightarrow H_2O + O_2 \qquad [R287]$$

The autoignition index is given by following definition, as detailed in [4].

$$AI = \left| \frac{\dot{w}_{HO_2}^{R287}}{\dot{w}_{HO_2}^{R287} + \dot{w}_{HO_2}^{R46}} \right| \tag{10}$$

Here, $\dot{w}_{HO_2}^{R287}$ stands for the contribution of reaction 287 to the reaction rate of HO_2 in the detailed reaction mechanism. Similarly, $\dot{w}_{HO_2}^{R46}$ is the contribution of reaction 46 to the reaction rate of HO_2.

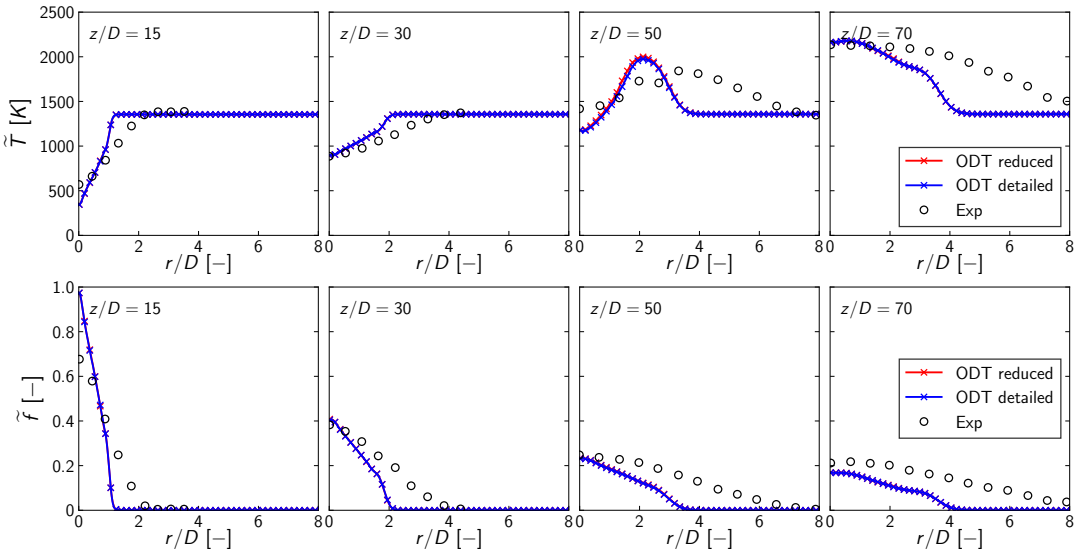

Figure 2. Radial profiles of Favre-averaged temperature and Favre-averaged mixture fraction from ODT simulations using a reduced and detailed reaction mechanism for the representation of the methane/air combustion. ODT results are compared to the experimental measurements of [1] (Exp).

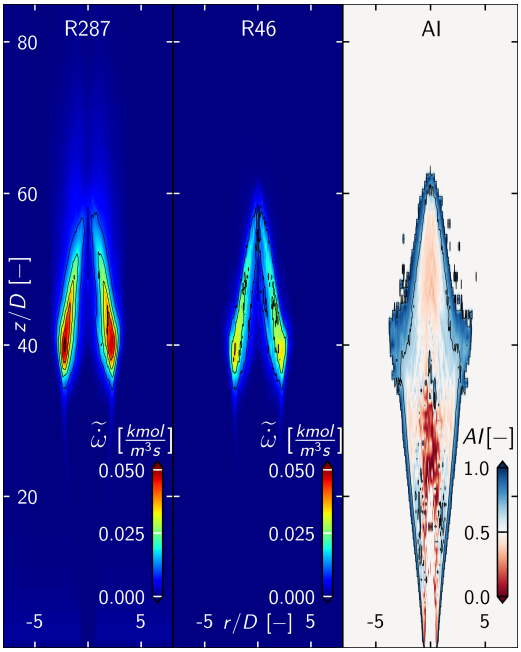

Figure 3. Two-dimensional renderings of the reaction rate of HO_2 of reaction 287, reaction rate of HO_2 of reaction 46, and mean autoignition index (AI). All results are averaged over the full ensemble size of ODT realizations.

Figure 3 illustrates the mean autoignition index, where blue regions (AI > 0.5) indicate autoignition-dominated zones, and red regions (AI < 0.5) represent propagation-dominated zones. In this visualization, propagation primarily occurs in the core of the flame, while autoignition is dominant in the transition region to the hot coflow. Compared to the instantaneous AI results from a 3-D LES simulation reported by [4] (not shown here), the ODT results exhibit similar spatial distributions of autoignition- and propagation-driven reaction zones. Given the reduced-order nature of the ODT model, its ability to provide insights into the autoignition index distribution while maintaining reasonable agreement with the findings of [4] highlights the effectiveness and potential of ODT.

4.4. Sensitivity to velocity and temperature variations

Figure 4 shows the sensitivity of the jet combustion to variations on jet velocity and coflow temperature. The centerline profiles for jet velocity variations reveal a later combustion with increasing jet velocity. This is indicated by a flatter temperature rise and more moderate oxygen consumption in the flame stabilization phase compared to the base case configuration with 100 m/s. A similar effect can be achieved by reducing the coflow temperature, as visible by the profiles for 1270 K, 1290 K, 1310 K, and 1330 K. However, with a higher temperature than the base case configuration of 1350 K, a faster combustion can also be observed. The temperature rise and oxygen consumption is thereby more rapidly. The mixture fraction, however, shows only minor differences between the profiles for different jet velocities and coflow temperatures. These findings are in well agreement with the parametric measurements of Cabra et al. [1] on the sensitivity of flame liftoff height to jet velocity and coflow temperature.

5. CONCLUSIONS

ODT simulation results for a lifted methane/air jet flame in an environment of hot combustion products have been presented. A cylindrical and temporal ODT formulation was employed using both a reduced and a detailed reaction mechanism, with

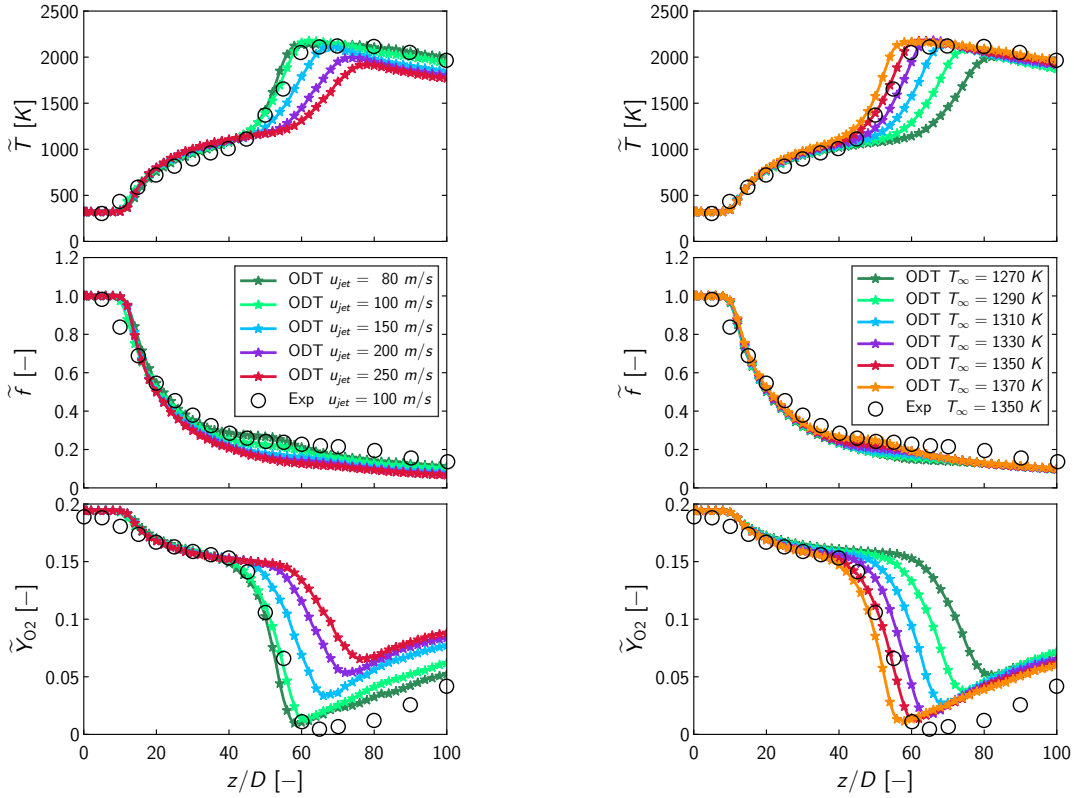

Figure 4. Centerline profiles of Favre-averaged temperature ($\tilde{T}$), mixture fraction ($\tilde{f}$), and oxygen mass fraction ($\tilde{Y}_{O2}$) from ODT simulations using a detailed reaction mechanism. Left: Sensitivity to jet velocity variations. Right: Sensitivity to coflow temperature variations.

comparisons made against the experimental measurements of [1]. The detailed mechanism consists of 53 species and 325 reactions, while the reduced mechanism includes 19 species and 15 reactions.

The comparison of centerline profiles with experimental data showed reasonable agreement for both reaction mechanisms, demonstrating ODT's ability to accurately reproduce Favre-averaged centerline profiles and their corresponding fluctuations. Additionally, the radial profiles for the pure mixing phase (z/D <30) aligned well with experimental observations. However, at positions further downstream (z/D >30), deviations from the experimental data were observed. The differences in the centerline and radial profiles between the detailed and reduced mechanism are negligibly small. The possibility of investigating the autoignition index and the influence of temperature and velocity variations reveals the benefits of the ODT model.

Overall, the results indicate that ODT successfully captures the essential combustion features of the investigated lifted methane/air jet flame in a vitiated coflow. Given its reduced-order nature, ODT proves to be an efficient and scale-resolving turbulence model for reactive jet flame simulations.

ACKNOWLEDGEMENTS

This research is supported by the German Federal Government, the Federal Ministry of Education and Research, and the State of Brandenburg within the framework of the joint project EIZ: Energy Innovation Center [project numbers 85056897 and 03SF0693A] with funds from the Structural Development Act (Strukturstärkungsgesetz) for coal-mining regions and the Brandenburg University of Technology (BTU) Graduate Research School [Conference Travel Grant].

REFERENCES

[1] Cabra, R., Chen, J.-Y., Dibble, R. W., Karpetis, A. N., and Barlow, R. S., 2005, "Lifted methane-air jet flames in a vitiated coflow", *Combustion and Flame*, Vol. 143, pp. 491–506.

[2] Domingo, P., and Vervisch, L., 2022, "Recent developments in DNS of turbulent combustion", *Proc Combust Inst*, Vol. 39 (2), pp. 2055–2076.

[3] Pope, S., 1985, "PDF methods for turbulent reactive flows", *Prog Energy Combust Sci*, Vol. 11 (2), pp. 119–192.

[4] Schulz, O., Jaravel, T., Poinsot, T., Cuenot, B., and Noiray, N., 2017, "A criterion to distinguish autoignition and propagation applied to a lifted methane–air jet flame", *Proceedings of the Combustion Institute*, Vol. 36 (2), pp. 1637–1644, URL https://www.sciencedirect.com/science/article/pii/S1540748916304114.

[5] Zhang, H., Yu, Z., Ye, T., Zhao, M., and Cheng, M., 2018, "Large eddy simulation of turbulent lifted flame in a hot vitiated coflow using tabulated detailed chemistry", *Applied Thermal Engineering*, Vol. 128, pp. 1660–1672, URL https://www.sciencedirect.com/science/article/pii/S1359431117316733.

[6] Domingo, P., Vervisch, L., and Veynante, D., 2008, "Large-eddy simulation of a lifted methane jet flame in a vitiated coflow", *Combustion and Flame*, Vol. 152 (3), pp. 415–432, URL https://www.sciencedirect.com/science/article/pii/S0010218007002519.

[7] Ihme, M., and See, Y. C., 2010, "Prediction of autoignition in a lifted methane/air flame using an unsteady flamelet/progress variable model", *Combustion and Flame*, Vol. 157 (10), pp. 1850–1862, URL https://www.sciencedirect.com/science/article/pii/S0010218010002038.

[8] Michel, J.-B., Colin, O., Angelberger, C., and Veynante, D., 2009, "Using the tabulated diffusion flamelet model ADF-PCM to simulate a lifted methane–air jet flame", *Combustion and Flame*, Vol. 156 (7), pp. 1318–1331, URL https://www.sciencedirect.com/science/article/pii/S0010218009000042.

[9] Gkagkas, K., and Lindstedt, R., 2007, "Transported PDF modelling with detailed chemistry of pre- and auto-ignition in CH4/air mixtures", *Proceedings of the Combustion Institute*, Vol. 31 (1), pp. 1559–1566, URL https://www.sciencedirect.com/science/article/pii/S1540748906003415.

[10] R. L. Gordon, A. R. Masri, S. B. P., and Goldin, G. M., 2007, "A numerical study of auto-ignition in turbulent lifted flames issuing into a vitiated co-flow", *Combustion Theory and Modelling*, Vol. 11 (3), pp. 351–376.

[11] Kerstein, A., 1988, "A Linear Eddy Model of Turbulent Scalar Transport and Mixing", *Combustion Science and Technology*, Vol. 60 (4-6), pp. 391–421.

[12] Kerstein, A. R., 2013, "Hierarchical parcel-swapping representation of turbulent mixing. Part 1. Formulation and scaling properties", *J Stat Phys*, Vol. 153 (1), pp. 142–161.

[13] Kerstein, A., 1999, "One-dimensional turbulence: model formulation and application to homogeneous turbulence, shear flows, and buoyant stratified flows", *Journal of Fluid Mechanics*, Vol. 392, pp. 277–334.

[14] Lignell, D., Lansinger, V., Medina M., J. A., Klein, M., Kerstein, A., Schmidt, H., Fistler, M., and Oevermann, M., 2018, "One-dimensional turbulence modeling for cylindrical and spherical flows: model formulation and application", *Theoretical and Computational Fluid Dynamics*, Vol. 32, pp. 495–520.

[15] Ashurst, W., and Kerstein, A., 2005, "One-dimensional turbulence: Variable-density formulation and application to mixing layers", *Physics of Fluids*, Vol. 17.

[16] McDermott, R., 2005, "Towards One-Dimensional Turbulence Subgrid Closure for Large-Eddy Simulation", Ph.D. thesis, University of Utah.

[17] Lignell, D., Kerstein, A., Sun, G., and Monson, E., 2013, "Mesh adaption for efficient multiscale implementation of One-Dimensional Turbulence", *Theoretical and Computational Fluid Dynamics*, Vol. 27 (3-4), pp. 273–295.

[18] Goodwin, D., 2002, *Cantera C++ User's Guide*, California Institute of Technology.

[19] Smith, G. P., Golden, D. M., Frenklach, M., Moriarty, N. W., Eiteneer, B., Goldenberg, M., Bowman, C. T., Hanson, R. K., Song, S., Gardiner, W. C., Lissianski, V. V., and Qin, Z., 1999, "http://www.me.berkeley.edu/gri_mech/", *Tech rep*.

[20] Lu, T., and Law, C., 2008, "A criterion based on computational singular perturbation for the identification of quasi steady state species: A reduced mechanism for methane oxidation with NO chemistry", *Combustion and Flame*, Vol. 154, pp. 761–774.

[21] Echekki, T., Kerstein, A., and Dreeben, T., 2001, "One-Dimensional Turbulence Simulation of Turbulent Jet Diffusion Flames: Model Formulation and Illustrative Applications", *Combustion and Flame*, Vol. 125, pp. 1083–1105.

[22] Bilger, R., S.H., S., and R.J., K., 1990, "On Reduced Mechanisms for Methane-Air Combustion in Nonpremixed Flames", *Combustion and Flame*, Vol. 80, pp. 135–149.